Gold-Assisted Deposition of a Material with Low Spitting by a New Carbon Removal Process

Taichi Ito, Kiyofumi Kodera, Yuichiro Shindo

Precious Metals Materials Division, Matsuda Sangyo Co., Ltd.

Shinjuku Nomura Building 6th Fl., 1-26-2 Nishishinjuku, Shinjuku-ku, Tokyo 163-0558, Japan

Tel: +81-3-3346-2319, E-mail: ito-t@matsuda-sangyo.co.jp

Keywords: Gold, Electron beam evaporation, Electron beam deposition, Au slugs, Au nodules, Au spitting

ABSTRACT

We developed a novel carbon-removing gas treatment process named "MNS" to reduce carbon contamination in Au evaporation sources during the swaging process for forming slug shapes. The MNS process with Au sources generated fewer carbon contaminants compared to the conventional Au source fabrication process. The process improvement was confirmed by SEM surface images and instrumental gas analysis. This reduction in contamination decreased the number of Au particles generated by carbon-derived spitting during evaporation by an order of magnitude. These results indicate the effectiveness of the MNS process to manufacture EB evaporation-source Au materials by significantly suppressing Au spitting.

INTRODUCTION

Electron-beam (EB) vacuum deposition is typically used to fabricate conducting metal electrodes for compound semiconductor devices. Au is one of the most commonly used metals for depositing thick conducting layers using EB. EB deposition was achieved using a multiple-crucible EB gun, which allowed a series of metals, such as Ti and Au, to be deposited sequentially in a vacuum chamber onto semiconductor wafers. Materials delivered to the hearth of the evaporation system are typically in the form of a slug (barrel or thick-diameter wire element), shot (granule), or wire (long-form narrow spool) to fill and replenish the EB crucibles for sequential vacuum deposition. Materials with a slug shape are popular for source replenishment because of their uniform shape and mass and their easy usage in managing the quantity of the replenished source.

Although these metals can be certified as 99.999% (5N) pure, mechanically formed shape materials such as slugs are often unavoidably contaminated during the refining and mechanical forming processes. Even though the incorporated carbon contaminants are at the parts-per-million (PPM) level, they float on the surface of the melted Au because of their lower density than that of Au [1-3]. Minute amounts of carbon contamination have been reported as a source of ballistic particulate generation (also called spitting) from an EB gun crucible during the heating, melting, and deposition steps. This is because electrons are reflected by the thin floating layer of high-melting-point carbon on the Au surface [1]. This floating carbon causes a thermal gradient across the floating carbon and the molten Au pool in the crucible. The thermal reactions at the edge of the floating agglomerated carbon on the molten Au pool originate from ballistic thermal spitting events. The Au particles generated by spitting affect the yield of the manufacturing process negatively if they are stacked on the surface of the MIM electrodes, source, or gate electrodes with very short spacing [1-3]. In addition, the reflected electrons affect the photoresist on the substrate. Because these back-scattering electrons have very high energy, their attack causes the photoresist layer to cross-link and is difficult to dissolve by a conventional wet strip process in a remover solution [3].

To avoid the undesired spitting of Au and curing of the photoresist, Au with a lower degree of carbon contamination is required for reliable and high-yield semiconductor manufacturing processes. As a solution to these problems, the adding of a small amount of Ta to the Au crucible has also been suggested to suppress Au spitting [3]. Ta can float on the surface of Au and form carbon because Ta is less dense than Au. However, this is not an essential solution for lowering the degree of carbon contamination. Therefore, we developed a new material processing method to reduce carbon contaminants and minimize short thermal ballistic (spitting) events. This processing method was named Matsuda New Evaporation Materials for Spitting Reduction (MNS) in this study.

EXPERIMENTAL PROCEDURE

The precious raw metal was melted in a carbon crucible, and the ingot underwent rolling, swaging, cutting, and cleaning to form barrel-shaped slugs. The MNS products were fabricated using an additional processing procedure different from that used for conventional industrially refined metal products. The products were treated with a special gas to enhance the removal of carbon and other volatile material

elements commonly found at the PPM level in the primary fabricated materials. The two types of Au sources were fabricated using two different manufacturing processes. Figure 1 shows the manufacturing process flowcharts for forming Au slugs with the conventional and MNS method, and Au slugs formed with these processes were named "Conventional-Au" and "MNS-Au" samples, respectively. The only difference between them is the application of the carbon removal process.

The surfaces of the conventional Au and MNS-Au slugs were observed using field-emission scanning electron microscopy (FE-SEM, JSM-7000F, JEOL Ltd.) and energy dispersive X-ray spectroscopy (EDX, Aztec Advanced Ultim Max40, Oxford Instruments) to evaluate carbon contamination on their surfaces.

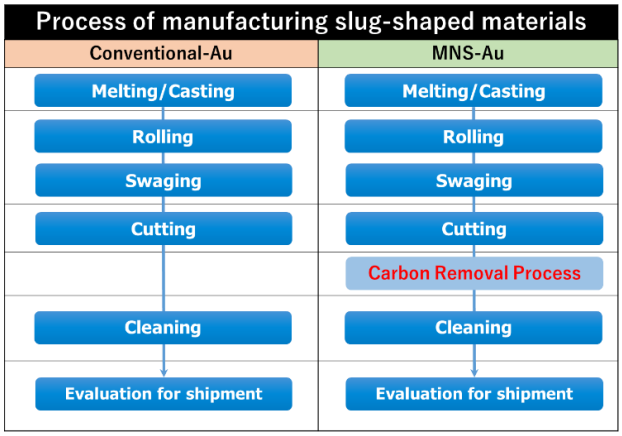

Fig. 1. Manufacturing process flowcharts for Conventional-Au and MNS-Au products.

A 150 nm Au thin film was deposited using an EB evaporator (SIP-700, Showa Vacuum) on 100 mmϕ Si wafers. The maintained deposition rate was 2 Å/s. The W crucibles were used as hearth liners for evaporation. Before depositing the Au thin film, a 20 nm-thick Ti thin film served as an adhesion layer. The W crucibles were removed from the vacuum chamber after finishing all the evaporation tests, and then the surface of the melted Au sources was observed by SEM to evaluate the surface floating carbon contamination originating from the melted Au slugs. The carbon content in both Au samples was measured using instrumental gas analysis (external analysis with CS844, LECO). A defect/particle inspection system (HYBRID C3, Lasertec) was used to measure the number of particles on the wafer. The resistivity of the deposited films was measured using the four-point probe method (Loresta-AX MCP-T370, Nittoseiko Analytech).

RESULT AND DISCUSSION

Figure 2 shows stereomicroscopic images of the Au slugs, and Figure 3 shows SEM images of the surface of the Au slug and the EDX analysis results. It is rigorous to find differences in surface contamination between conventional Au and MNS-Au by stereomicroscopic inspection of their surfaces, which revealed the many black spots on the conventional Au slug. These black spots were confirmed by EDX analysis, as carbon contamination was observed on the surface of the Au slug. However, no evident adhesion of carbon was observed on the surface of MNS-Au.

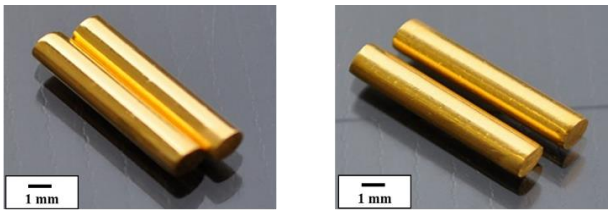

(a) Conventional-Au **(b) MNS-Au**

Fig. 2. Surface stereomicroscope images of Conventional-Au (a), and MNS-Au (b).

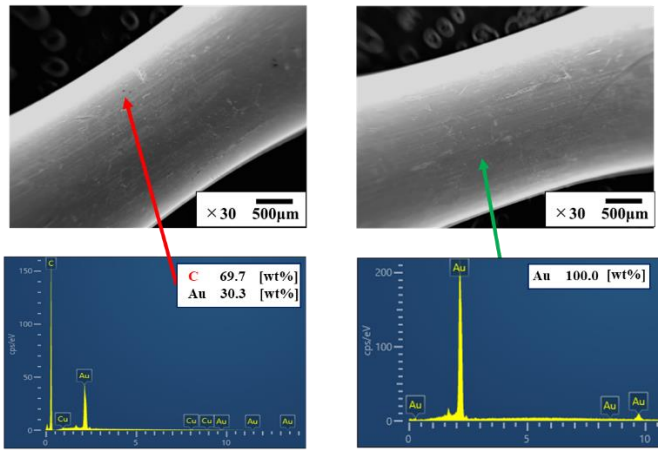

(a) Conventional-Au **(b) MNS-Au**

Fig. 3. SEM images and EDX spectrum acquired at the surface of Conventional-Au (a) and MNS-Au (b).

Figure 4 shows the cross-sectional SEM images and EDX results measured on the cross-sections of the conventional Au and MNS-Au slugs. Many carbon particles are embedded in a conventional Au slug, with higher density near the surface of the slug. Inside the MNS-Au slugs, there were fewer carbon particles, as determined from the cross-sectional SEM images. These results indicate that the carbon-removal treatment introduced in the MNS-Au fabrication process was very effective in reducing carbon contamination on and near the surface of the Au slug.

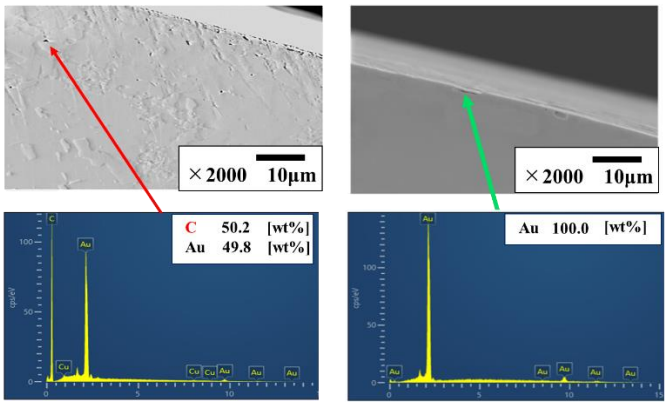

(a) Conventional-Au **(b) MNS-Au**

Fig. 4. SEM images and EDX spectrum acquired at cross-section of Conventional-Au slug (a) and MNS-Au slug (b). EDX analysis was carried out at the points indicated by allows.

Figure 5 shows the stereomicroscope and SEM images of the surface of the Au melts that were removed from the hearth liner in the vacuum chamber of the EB evaporation system after evaporation. As can be easily seen from the stereomicroscopic image of the conventional Au melt, large areas of the surface of the Au melt are covered with black residues large enough to be checked. In previous works [1-3], these black residues originated from carbon particles embedded inside the source Au materials. Using the same analogy, it can be interpreted that embedded carbon particles inside conventional Au slugs were released and floated up to the surface of molten Au when their slugs had been melted and formed into molten Au by high-energy electron beams from an e-gun. This reaction finally resulted in condensed visible-scale black residues on the surface of the Au melt. However, the surface of the Au melt formed with MNS-Au was shiny and clean, with no visible black carbon residues. This difference was confirmed by microscopic range inspection with SEM as electron microscopy and stereomicroscopy.

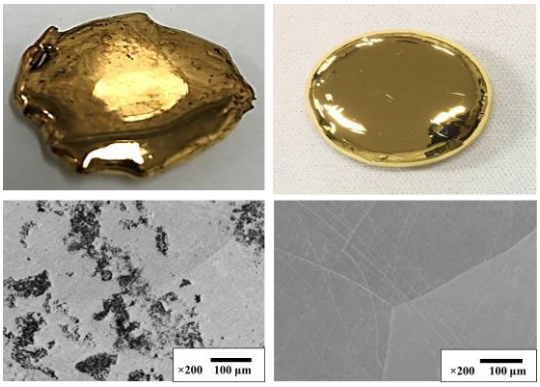

(a) Conventional-Au **(b) MNS-Au**

Fig. 5. Stereomicroscope images and SEM images of the surface of Au melts of Conventional-Au (a) and MNS-Au (b)

Figure 6 shows the magnified SEM images and EDX mapping results observed at the surface of the Au melts of conventional Au (a) and MNS-Au (b). EDX maps were obtained for carbon atoms. For the surface of the conventional Au melt, the emphasized bright red-colored parts correspond to areas containing a high quantity of carbon. In contrast, the surface carbon distribution level of the MNS-Au melt corresponds to the baseline level of conventional Au, and there is no bright red high-carbon-contaminated area throughout the mapping area.

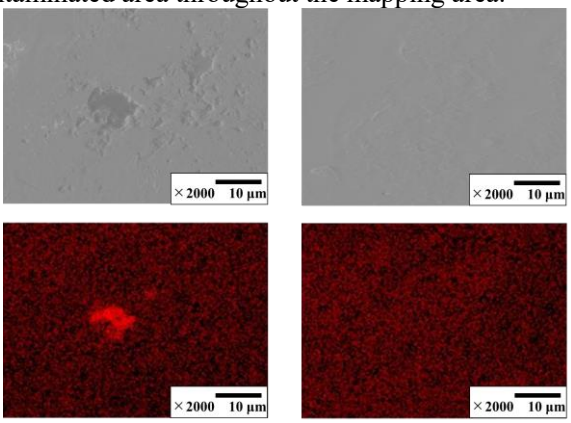

(a) Conventional-Au **(b) MNS-Au**

Fig. 6. Magnified SEM images and EDX mapping measurement results observed at the surface of Au melts of Conventional-Au (a) and MNS-Au (b). EDX maps were obtained for the carbon atom.

The average carbon contents of the conventional Au and MNS-Au melts measured by instrumental gas analysis are shown in Figure 7. These are the average values of four melt samples for each Au source. The carbon content of the MNS-Au melt source was reduced to approximately two-thirds that of the conventional Au melt.

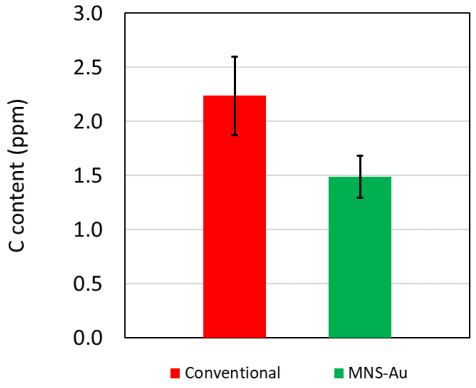

Fig. 7. Comparison of the average carbon content of the Conventional-Au and MNS-Au melts analyzed by instrumental gas analysis

Figure 8 shows one of the particle maps of the Au thin-film-deposited wafers evaluated using a defect/particle inspection system. At a glance, it can be found that the number of

particles of Au nodules was drastically improved when MNS-Au was used as source material. The defect/particle inspection system is capable of counting particles that are the size of 1-400 μm^2. The total number of particles from the three runs of conventional Au and MNS-Au deposition is summarized in Table 1. The number of nodules in the MNS-Au-deposited wafers substantially decreased to approximately one-twentieth of that of conventional Au. This improvement in Au nodule generation by Au spitting can be attributed to the reduction of carbon contamination using the proposed MNS process.

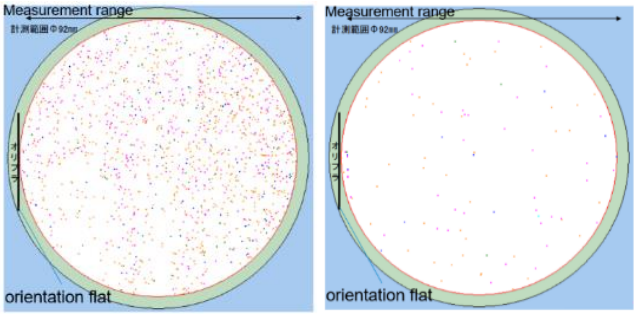

(a) Conventional-Au **(b) MNS-Au**

Fig. 8. Particle maps of Au thin film deposited wafers

TABLE 1
THE NUMBER OF NODULES ON CONVENTIONAL-AU AND MNS-AU DEPOSITED WAFERS

	Number of nodules in Si wafer	
	Conventional-Au	MNS-Au
Wafer ①	1,564	109
Wafer ②	2,117	119
Wafer ③	2,385	79
The average number of nodules	2,022	102

Finally, we evaluated the specific electrical resistivity of the Au films deposited with conventional Au and MNS-Au slugs. The specific electrical resistivity was measured at 17 points in the horizontal and vertical directions relative to the flat orientation. Figure 9 shows the average values of the specific electrical resistance of three Au-deposited wafers with conventional Au and MNS-Au slugs.

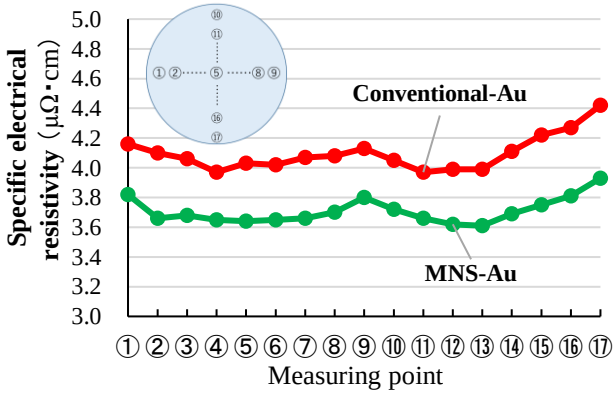

Fig. 9. Specific electrical resistivity of Au deposited wafer with Conventional-Au and MNS-Au samples.

A comparison of the specific electrical resistivities of the conventional Au- and MNS-Au-deposited films confirmed that the MNS-Au-deposited films had a lower specific electrical resistivity than the conventional Au-deposited films. In this study, although we did not investigate the quantitative relationship between the carbon impurity concentration and the specific electrical resistivity, it is possible that the use of lower carbon-contaminated slugs lowers the specific electrical resistivity because the impurity concentration of Au generally affects the specific electrical resistivity.

CONCLUSIONS

Comparing the MNS process adopted by Au slugs and that made by the conventional method, surface and cross-sectional SEM observation, and EDX analysis revealed that surface adhesion and embedded carbon particles near the surface of the slug were drastically reduced for Au slugs made with the MNS process. The Au melts used for the EB evaporation processes also showed the effectiveness of the application of the MNS process because of less carbon adhesion and corroborative evidence of lower carbon content measured by instrumental gas analysis.

A defect/particle inspection system was used to evaluate the number of Au nodules deposited on the wafer surface owing to Au spitting and verify the relationship between the carbon content in the Au slug and the occurrence of Au spitting. The average total number of particles counted from three runs with the MNS process-applied slugs substantially decreased to approximately one-twentieth of that using the conventional process-applied slugs. In addition, the specific electrical resistivity measurement results indicate that the Au thin film deposited with a lower carbon-contaminated MNS-processed slug has a lower specific electrical resistivity. These results show that the MNS-Au process, our new carbon removal process, is very effective for manufacturing Au slugs as EB evaporation sources to improve Au spitting.

ACKNOWLEDGEMENTS

The authors would like to thank the scientists and engineers of Ferrotec (USA) Corporation's Temescal Division for their support, communication, and helpful discussions over the past four years.

REFERENCES

[1] K. Cheng, "*Electron Radiation as an Indicator of Gold Nodule Defect during E-beam Evaporation"*, CS Mantech Conference 2011

[2] J. Cotronakis, M.Clarke, R. Lawrence, J. Campbell and C. Gaw, "*Continuous Directivity Improvements and Impact on High Density Metal-Insulator-Metal (HDMIM) Capacitor Yields*", CS Mantech Conference 2004

[3] K. Cheng, D. Mitchell, M. Le and L. Hans, "*Effect of electron radiation generated during E-beam evaporation on a photoresist liftoff process*", CS Mantech Conference 2010.